Velocity analysis using similarity-weighted semblance[a]

[a]Published in Geophysics, 80, A75-A82, (2015)

Yangkang Chen, Tingting Liu† and Xiaohong Chen†*

ABSTRACT

Weighted semblance can be used for improving the performance of the traditional semblance for specific datasets. We propose a novel approach for prestack velocity analysis using weighted semblance. The novelty comes from a different weighting criteria in which the local similarity between each trace and a reference trace is used. On one hand, low similarity corresponds to a noise point or a point indicating incorrect moveout, which should be given a small weight. On the other hand, high similarity corresponds to a point indicating correct moveout, which should be given a high weight. The proposed approach can also be effectively used for analyzing AVO anomalies with increased resolution compared with AB semblance. Both synthetic and field CMP gathers demonstrate higher resolution using the proposed approach. Applications of the proposed method on a prestack dataset further confirms that the stacked data using the similarity-weighted semblance can obtain better energy-focused events, which indicates a more precise velocity picking.

INTRODUCTION

Building a subsurface velocity model is one of the most important issues in exploration geophysics. There are generally four ways for building the velocity model. The first one is normal-moveout (NMO) based velocity analysis, which requires picking peaks in the velocity spectra (Taner and Koehler, 1969; Fomel, 2009; Luo and Hale, 2012). The velocity spectra is obtained by applying a number of NMO corrections with different velocities and then calculating their corresponding semblances. The second type is Born-approximation-based wave equation migration velocity analysis (WEMVA), which is a non-linear optimization process that aims at estimating the migration velocity using the Born-approximated wave equation in the image domain and is less vulnerable to the local minimum and more effective for reflection signals (Sava and Biondi, 2004a,b; Li, 2013). The third type is ray-based migration velocity analysis, also known as traveltime tomography. The velocity model is built by updating the velocity model so that the misfit between predicted and observed first-break traveltimes is minimized (Zhu et al., 1992; Osypov, 2000; Noble et al., 2010; Li et al., 2013; Chen et al., 2013). The fourth type is the recently popular full waveform inversion (FWI), which minimizes the least-squares misfit between the measured data and the synthesized data predicted from the current velocity model in the data domain (Virieux and Operto, 2009; Guitton et al., 2012; Zhou et al., 2012) and can improve the resolution of velocity structures. In this paper, we focus on the NMO based velocity analysis , which provides the important initial velocity model for the following more complicated velocity analysis procedures.

NMO based velocity analysis using semblance has been an indispensable step for building the initial subsurface velocity model since its introduction by Taner and Koehler (1969). There exist several modifications of traditional semblance that better meet the requirements of specific datasets (Fomel, 2009; Sarkar et al., 2001; Luo and Hale, 2012). Sarkar et al. (2001) and Fomel (2009) modified the traditional semblance formulation and proposed amplitude-versus-offset (AVO) adaptive semblances in different ways. Luo and Hale (2012) increase the resolution of the semblance map in order to distinguish the peaks between primary and multiple reflections.

Increasing the resolution of the semblance spectra is beneficial for picking the true NMO velocity, especially important when multiples are existing in the CMP gathers (Luo and Hale, 2012). We can increase the resolution by weighting terms in the traditional semblance calculation. Hale (2009) defined a weighted semblance that conformed to structural features. Luo and Hale (2012) chose an offset-dependent weighting function that effectively increased the semblance spectra resolution. In this paper, we use a different weighting scheme, by utilizing the local similarity between each trace and a reference trace. The reference trace can be a zero-offset trace, or the stacked trace using a traditional stacking technique. Both synthetic and field data examples demonstrate a successful performance of the proposed approach.

THEORY

Traditional semblance

The traditional semblance is defined by Neidell and Taner (1971) as:

$$s(i) = \frac{\sum_{j=i-M}^{i+M} \left(\sum_{k=0}^{N-1} a(j,k) \right)^2}{N \sum_{j=i-M}^{i+M} \sum_{k=0}^{N-1} a^2(j,k)}, \tag{1}$$

where i and j are time sample indices, $s(i)$ denotes the semblance for time index i, $2M+1$ is the length of the smoothing window (in this formulation a boxcar filter is used), along time axis, $a(j,k)$ is the trace amplitude at time index j and trace number k of the NMO-corrected common midpoint (CMP) gather, and N is the number of traces.

Weighted semblance

The semblance can be thought as a squared correlation between the analyzed signal and a weighting function $w(j,k)$ in the following form:

$$s_w(i) = \frac{\sum_{j=i-M}^{i+M} \left(\sum_{k=0}^{N-1} a(j,k) w(j,k) \right)^2}{\sum_{j=i-M}^{i+M} \left(\sum_{k=0}^{N-1} a^2(j,k) \sum_{k=0}^{N-1} w^2(j,k) \right)}, \tag{2}$$

where $w(j,k)$ denotes the weighting function for time index j and trace number k.

With w selected using different criterion, equation 2 can lead to different well-known semblance types:

1. When $w(j,k) \equiv C$, where C is a constant, equation 2 turns to the traditional semblance 1.
2. When $w(j,k) = A(j) + B(j)\phi(j,k)$, where $\phi(j,k)$ is a known function, $A(j)$ and $B(j)$ are two coefficients estimated from the least-squares fitting for the trend function $w(j,k)$, equation 2 turns to the AB semblance proposed by Fomel (2009). The AB semblance is proposed to handle the velocity analysis for those CMP gathers with AVO phenomenon. Appendix A provides a short review of calculating $A(j)$ and $B(j)$ in the AB semblance.

More recently, Luo and Hale (2012) proposed another weighting approach which honors the large-offset data and damping the small-offset data to increase the resolution for the resulted velocity scanning map. In this abstract, we propose to use local similarity (Fomel, 2007) to weight different traces:

$$w(j,k) = \mathbf{S}[a(j,k), r(j)], \tag{3}$$

where $\mathbf{S}[\mathbf{x},\mathbf{y}]$ denotes the local similarity between traces $\mathbf{x}$ and $\mathbf{y}$, $r(j)$ denotes the jth time point for a selected reference trace $\mathbf{r}$. The reference can be easily selected as the zero-offset trace, or more plausible, as the stacked trace using the conventional stacking technique or a more sophisticated stacking technique (Liu et al., 2009). In most cases, when the signal-to-noise ratio (SNR) of the CMP gather is not low, the choice of reference trace will not affect the performance too much. However, when the CMP gather is very noisy, the stacked trace using a better stacking technique can help obtain a better focused and smoother semblance map.

Figure 1 gives a brief demonstration of the proposed similarity-weighted semblance. Figure 1a is a simple NMO corrected CMP gather with some Gaussian white noise. There are two abnormal traces in the gather. For traditional semblance, the two abnormal traces are given equal weights, which is not plausible. Figure 1b shows the weights applied to each trace for the semblance calculation. The weights equal to the local similarity between each trace and the stacked trace. As we can see from the map of weights, the two abnormal traces are given much low weights. The more reasonable semblance calculation will result in a much higher resolution, which will be exclusively demonstrated in the section of examples. In the next section, we will give a brief review of the theory of local similarity.

REVIEW OF LOCAL SIMILARITY

Fomel (2007) defined local similarity between vectors $\mathbf{a}$ and $\mathbf{b}$ as:

$$\mathbf{c} = \sqrt{\mathbf{c}_1^T \mathbf{c}_2} \tag{4}$$

where $\mathbf{c}_1$ and $\mathbf{c}_2$ come from two least-squares minimization problems:

$$\mathbf{c}_1 = \arg\min_{\mathbf{c}_1} \|\mathbf{a} - \mathbf{B}\mathbf{c}_1\|_2^2, \tag{5}$$

$$\mathbf{c}_2 = \arg\min_{\mathbf{c}_2} \|\mathbf{b} - \mathbf{A}\mathbf{c}_2\|_2^2, \tag{6}$$

where $\mathbf{A}$ is a diagonal operator composed from the elements of $\mathbf{a}$: $\mathbf{A} = diag(\mathbf{a})$ and $\mathbf{B}$ is a diagonal operator composed from the elements of $\mathbf{b}$: $\mathbf{B} = diag(\mathbf{b})$. Least-squares problems 5 and 6 can be solved with the help of shaping regularization with a smoothness constraint:

$$\mathbf{c}_1 = [\lambda_1^2\mathbf{I} + \mathcal{T}(\mathbf{B}^T\mathbf{B} - \lambda_1^2\mathbf{I})]^{-1}\mathcal{T}\mathbf{B}^T\mathbf{a}, \tag{7}$$

$$\mathbf{c}_2 = [\lambda_2^2\mathbf{I} + \mathcal{T}(\mathbf{A}^T\mathbf{A} - \lambda_2^2\mathbf{I})]^{-1}\mathcal{T}\mathbf{A}^T\mathbf{b}, \tag{8}$$

where $\mathcal{T}$ is a smoothing operator, and λ_1 and λ_2 are two parameters controlling the physical dimensionality and enabling fast convergence when inversion is implemented iteratively. These two parameters can be chosen as the least-squares norms of $\mathbf{B}$ and $\mathbf{A}$, respectively.

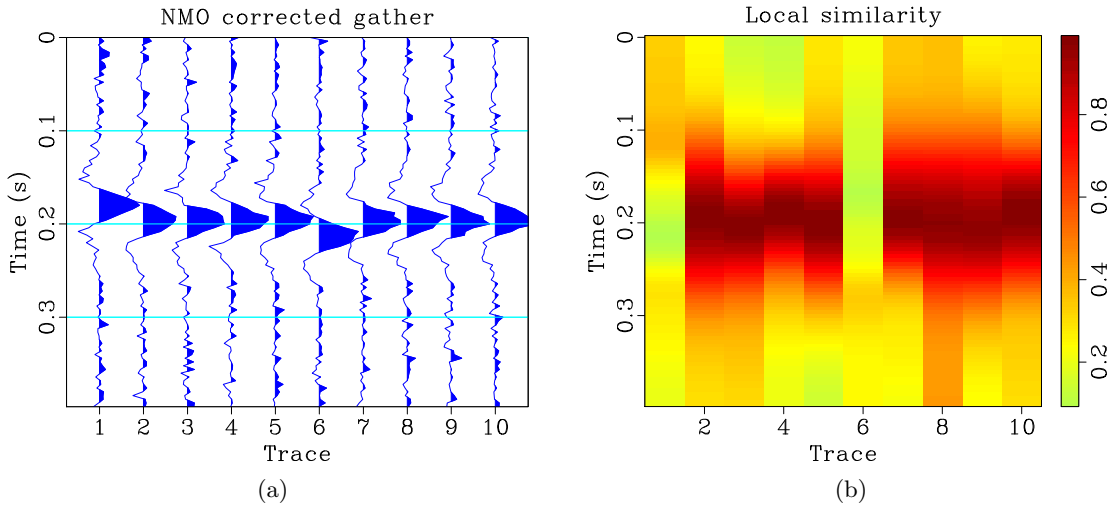

Figure 1: A demonstration of similarity-weighted semblance. (a) NMO corrected gather. (b) Weights applied to each trace for semblance calculation based on the local similarity between each trace and a reference trace. weight/ syn,weights

EXAMPLES

Synthetic examples

The first synthetic example is a simple four-layer hyperbolic CMP gather. By using the traditional semblance, AB semblance and the proposed similarity-weighted semblance, the semblance spectra are shown in Figure 2. From the comparison, we can see that the resolution is clearly different for three approaches. The AB semblance suffers from the low-resolution problem as pointed out by Fomel (2009), compared with the other two approaches. For both traditional and AB semblances, there exists a fake peak between the third and fourth layer. The similarity-weighted semblance obtains a very high resolution both vertically and horizontally. In this example, the reference trace is chosen as the traditionally stacked trace.

By adding some Gaussian white noise onto the first synthetic example, we get the second example (Figure 3). The performance of the three approaches are improved a lot due to the added random noise. The fake peaks appearing in the first example disappear because of the random property of Gaussian white noise, which indicates the fact that a small level of

random noise can aid the semblance calculation process to some extent. Compared with the other two approaches, the similarity-weighted semblance obtained a very high resolution. In this example, the reference trace is chosen as the traditionally stacked trace.

The third synthetic example is a CMP gather with class II AVO anomalies (Figure 4). The class II AVO anomalies cause seismic amplitudes to go through a polarity reversal (Rutherford and Williams, 1989; Fomel, 2009). In this test, the weighting function is a combination between the similarity based weight and trend based weight. We implement this by first weighting each trace using the proposed approach and then apply the trend based approach (Fomel, 2009). While the traditional semblance can not capture the information of the AVO anomalies, the AB semblance and the proposed similarity-weighted semblance can handle the AVO phenomena correctly. Because of the combination between the AB semblance and similarity-weighted semblance, the resolution of the proposed approach will decrease a little bit. This phenomenon results from the fact that taking AVO effect into consideration will decrease the resolution, as analyzed in Fomel (2009). However, the resolution using the proposed approach is still higher than that of the AB semblance and comparable to the traditional semblance. In this example, the reference trace is chosen as the traditionally stacked trace.

It's worth to be mentioned that the black strings appearing on the top of velocity maps denote the automatically picked optimum velocities using the algorithm introduced in Fomel (2009). Thus, the trends of black strings between different semblance approach do not differ too much. With manual picking, the results for both traditional semblance and AB semblance will result much larger velocity uncertainties, which will result in larger migration uncertainties (Fomel and Landa, 2014). There are also some unreasonable changes in the black strings, which result from the fact that the synthetic events are sparse and the automatically picking algorithms can not handle such problem. Figure 5 shows a comparison between the true velocity and the picked velocities from different approaches for the third synthetic example. The black solid line denotes the true velocity. The blue dash line denotes the picked velocity using the similarity-weighted semblance. The green long dash line denotes the picked velocity from the traditional semblance and the red dot dash line denotes the picked velocity from the AB semblance. It is clear that the AB semblance and similarity-weighted semblance are much similar and the similarity-weighted semblance can make the automatic picking more accurate. The velocity picked from the traditional semblance, however, deviates the true velocity a lot and is not acceptable.

Field data examples

The first field data is a marine CMP gather (Figure 6). In this example, the proposed similarity-weighted semblance as shown in the right panel in Figure 6 obtains a very high resolution. The peaks on the semblance panel is easy to be picked out and thus reduce the velocity-peaking uncertainties (Fomel and Landa, 2014). In this example, the reference trace is chosen as the stacked trace using the SNR-weighting strategy.

The second field data example is a 3D prestack dataset from a 2D survey of the Gulf of Mexico, as shown in Figure 7. We stacked the prestack data using automatically picked NMO velocities from different semblance map. Figure 8a shows the stacked data using traditional semblance and Figure 8b shows the stacked data using the similarity-weighted

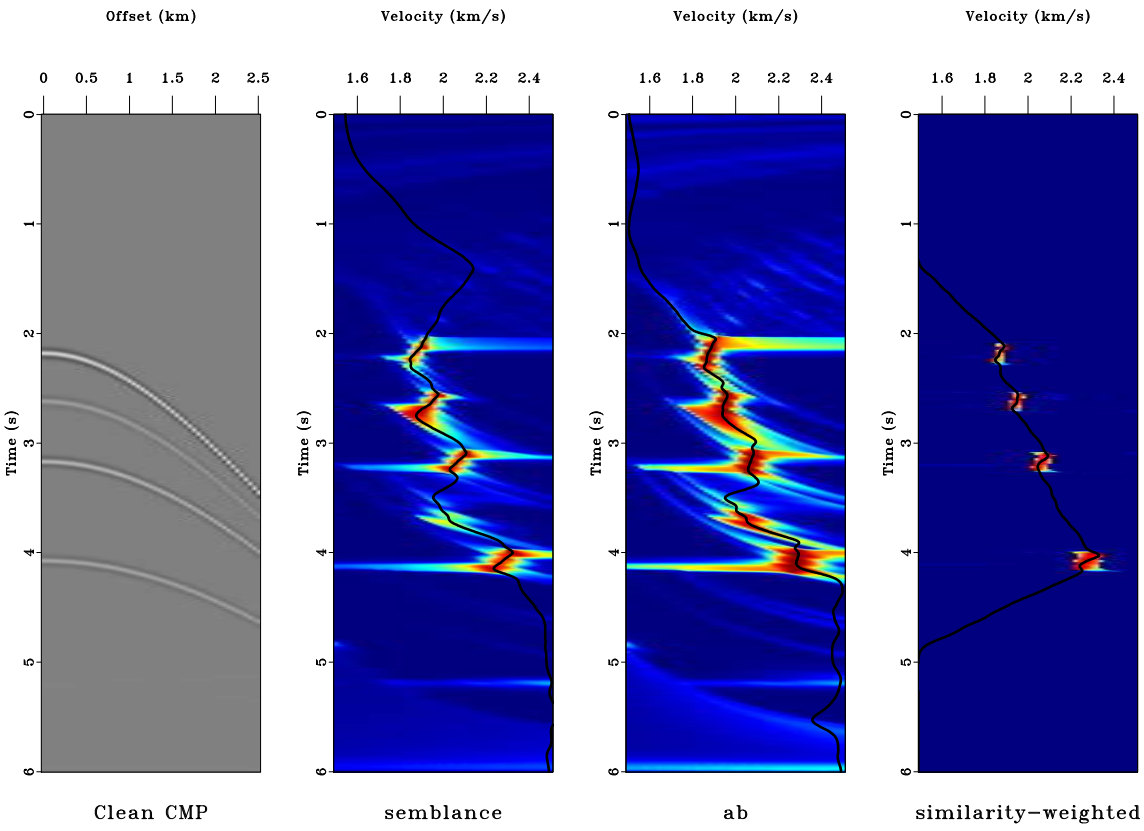

Figure 2: Comparison between semblance spectra for a clean synthetic data. Left: CMP gather. Middle left: using traditional semblance. Middle right: using AB semblance. Right: using similarity-weighted semblance. hw/ hw-comp1

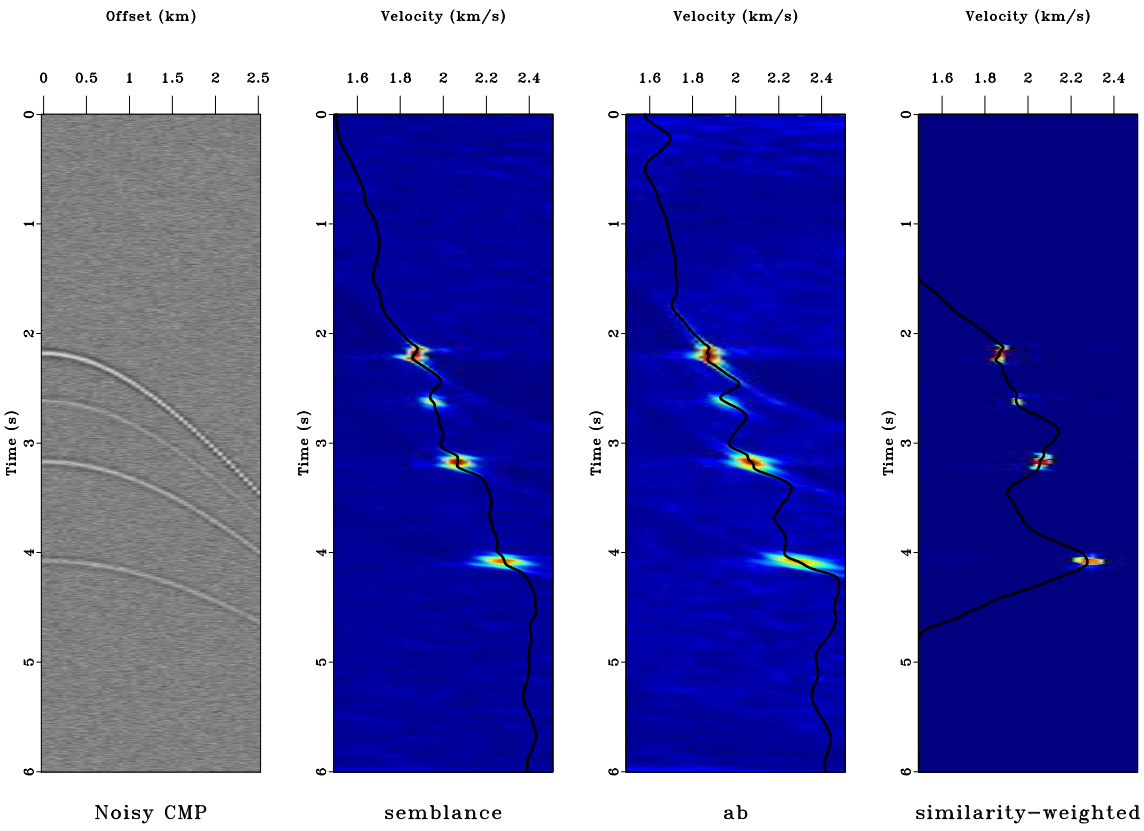

Figure 3: Comparison between semblance spectra for a noisy synthetic data. Left: CMP gather. Middle left: using traditional semblance. Middle right: using AB semblance. Right: using similarity-weighted semblance. hw/ hw-comp2

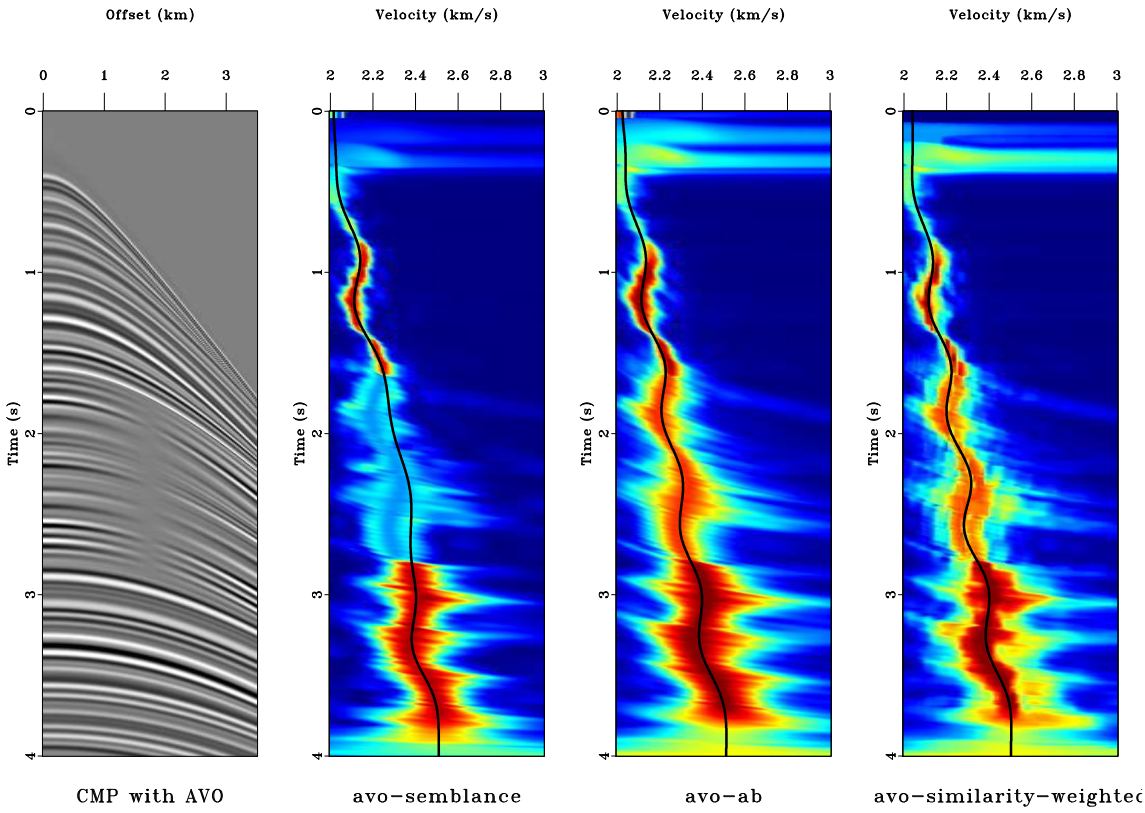

Figure 4: Comparison between semblance spectra for a synthetic data with class II AVO anomalies. Left: CMP gather. Middle left: using traditional semblance. Middle right: using AB semblance. Right: using similarity-weighted semblance. synth/ synth-comp2

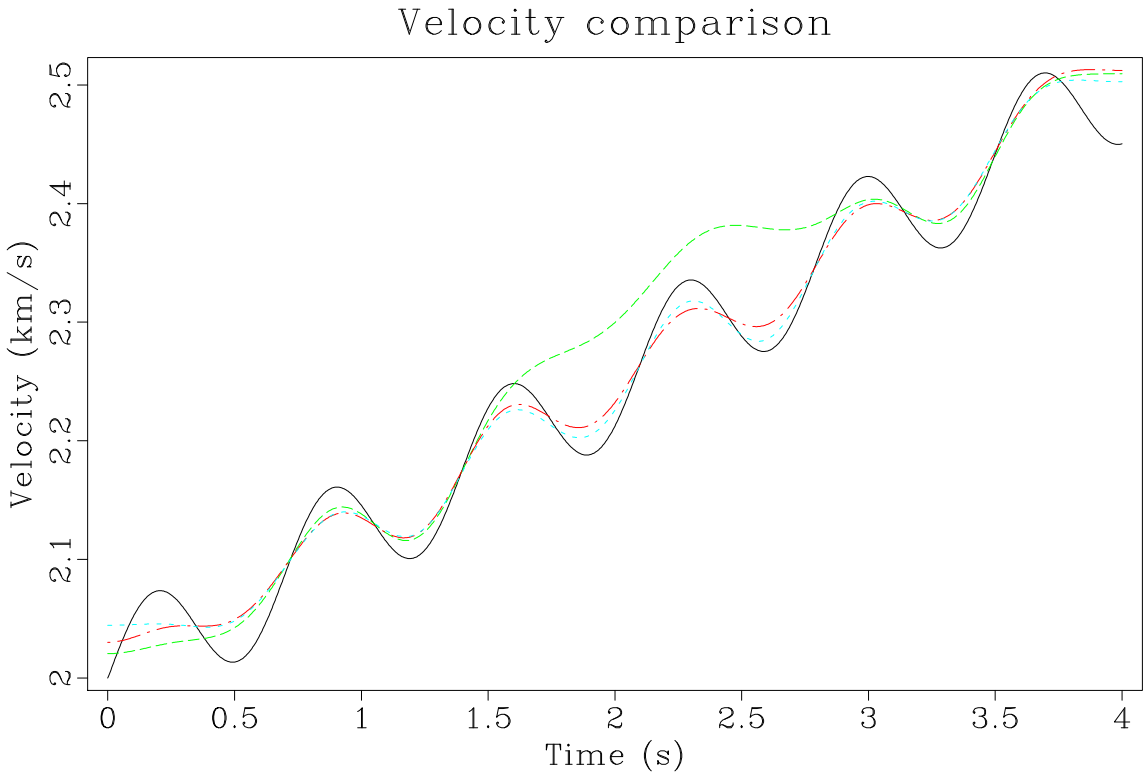

Figure 5: Comparison between the true velocity and picked velocities for the third synthetic example with class II AVO anomalies. Black solid line denotes the true velocity. Green long dash line corresponds to the picked velocity by traditional semblance. Red dot dash line corresponds to the picked velocity by AB semblance. Blue dash line corresponds to the picked velocity by similarity-weighted semblance. synth/ vcomp

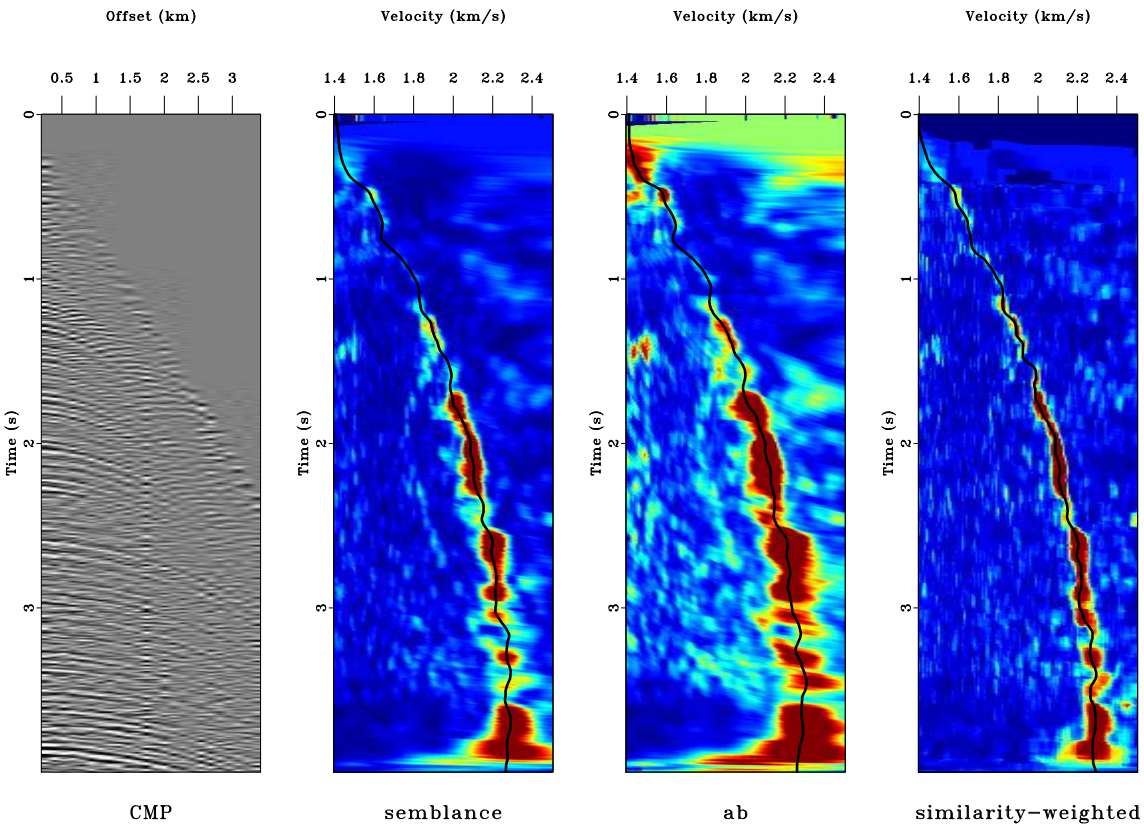

Figure 6: Comparison between semblance spectra for field data. Left: CMP gather. Middle left: using traditional semblance. Middle right: using AB semblance. Right: using similarity-weighted semblance. bei/ comp1

semblance. The stacked data using the proposed approach can obtain better stacked result with stronger stacked energy, which indicates a more precise picked velocity. The comparison between Figures 8a and 8b is not very obvious. However, when we zoomed two parts from the original stacked sections, as shown in Figures 8c and 8d, we can find significant improvement. The two zoomed parts are highlighted by the two frame boxes in Figures 8a and 8b. In this example, the reference trace is chosen as the traditionally stacked trace.

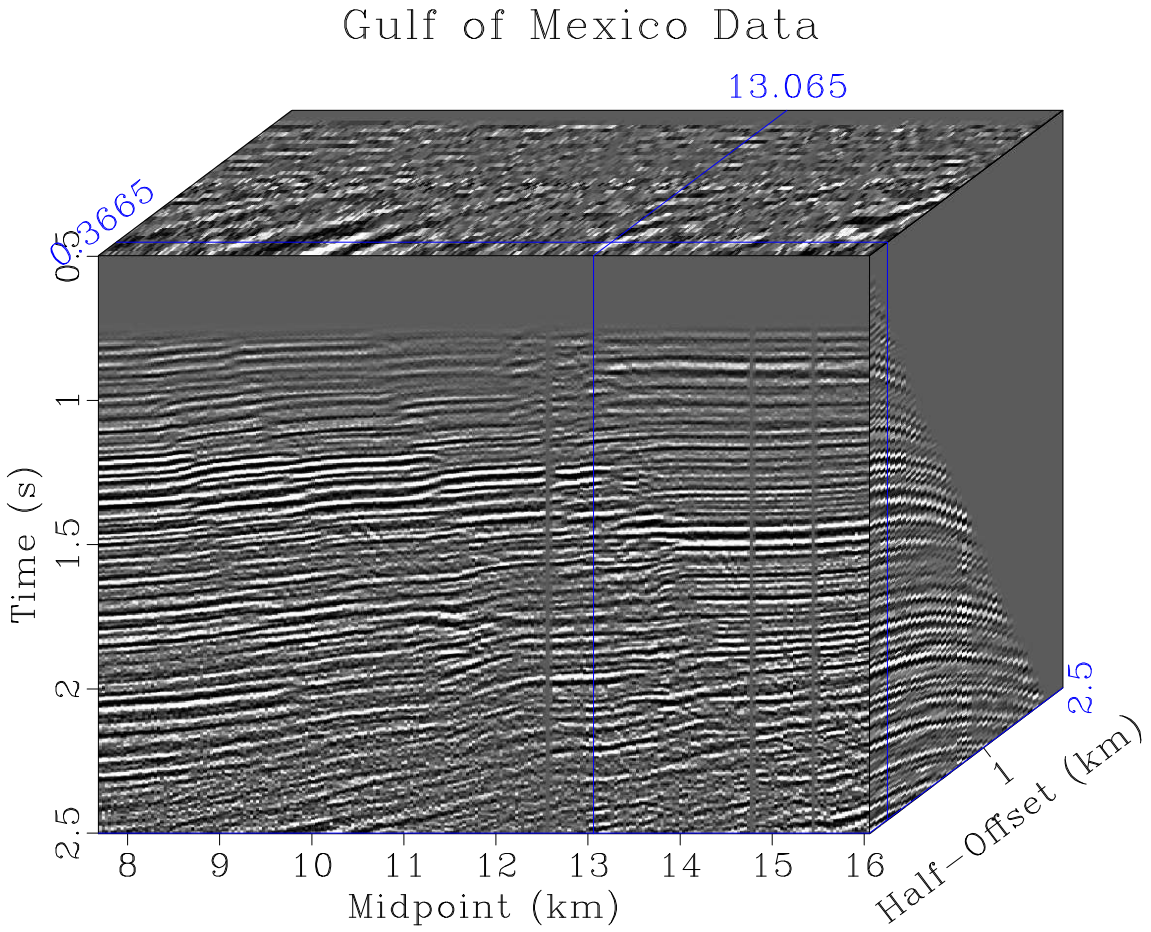

Figure 7: A prestack dataset from the Gulf of Mexico. stack/ gulf

DISCUSSION

Velocity analysis is of exceptional importance to the whole seismic data processing tasks and the NMO based velocity picking can provide the very initial velocity model for all the other velocity analysis approaches. Most of the current velocity-picking procedures are based on manual endeavors and the resolution of the velocity spectrum greatly affects the finally picked velocity. The above two reasons make the subject of this paper significant. Even with automatic picking algorithms, the proposed similarity-weighted semblance can still be superior than the traditional semblance, which has been demonstrated by the third synthetic and the second field data examples.

When implementing the proposed algorithm, we also need to calculate the traditional

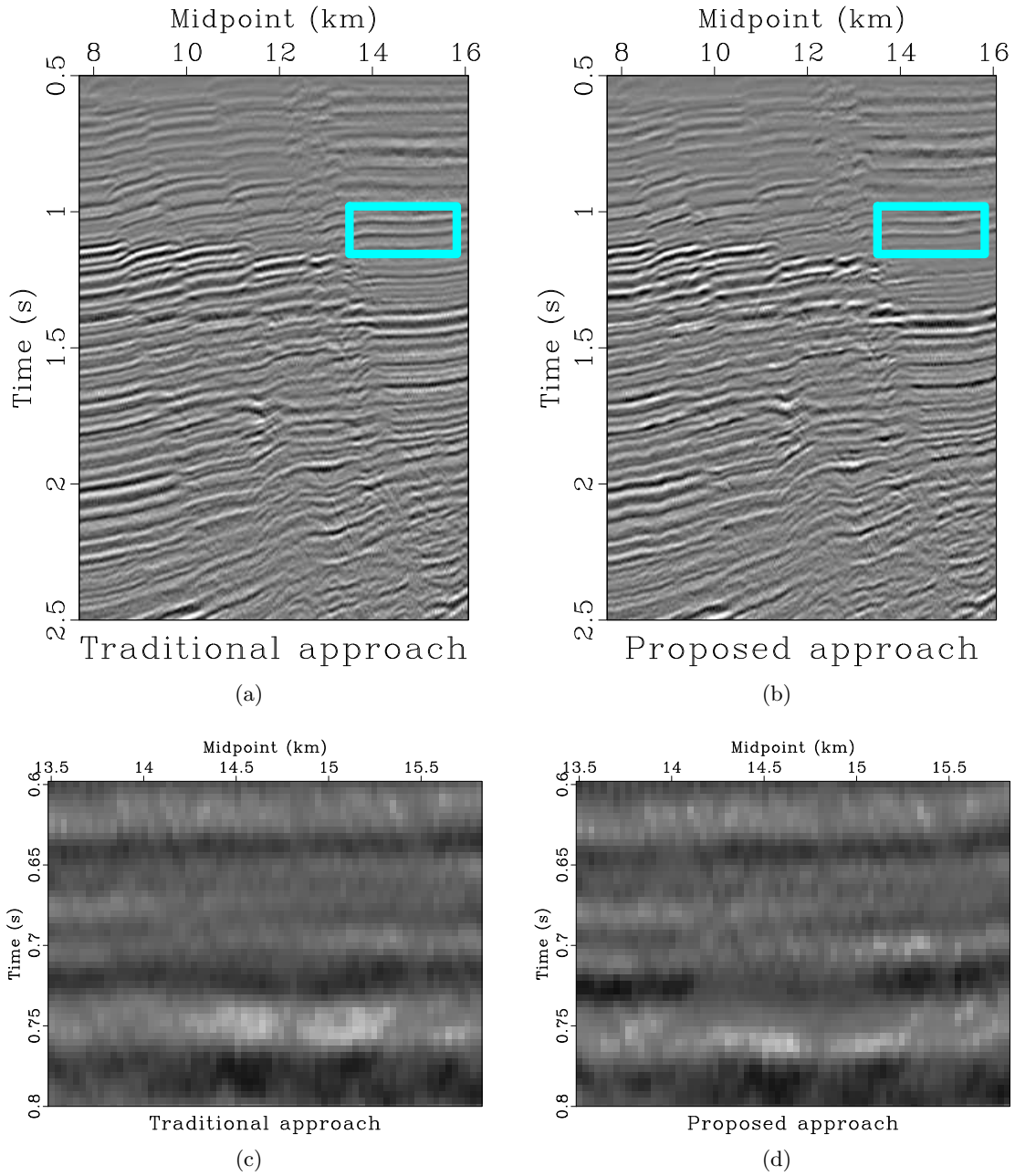

Figure 8: (a) Stacked data using automatically picked NMO velocity from the traditional semblance. (b) Stacked data using automatically picked NMO velocity from the similarity-weighted semblance. (c) Zoomed section from (a). (b) Zoomed section from (b). The two zoomed parts are highlighted by the frame boxes in (a) and (b). stack/ stack,simistack,stack-A,simistack-A

semblance in order to obtain a stacked reference trace. The inappropriate traditional stacking result will result in inappropriate calculation of the similarity-weighted semblance. In practice, we need to iterate several times to obtain an acceptable reference trace. Because of the iteration and the calculation of the local similarity, the proposed semblance will have some extra computational cost. However, the computational efficiency is still acceptable, and considering that the semblance calculation can be parallelized CMP by CMP, the computational cost is not a serious issue.

The proposed similarity-weighted semblance can be conveniently implemented based on the traditional semblance calculation framework. The only change is to weight each trace using the local similarity. The local similarity is a robust local attribute that can be easily calculated and has found many applications in exploration geophysics field (Liu et al., 2009; Chen and Fomel, 2015). Thus, the proposed approach has the potential to be widely used in the industry.

CONCLUSIONS

We have proposed a general formulation for the weighted semblance. The traditional semblance is no more than a weighted semblance with constant weight. The AB semblance corresponds to a weighted semblance with a trend function derived from the data. With a weighting function using the local similarity between each trace and a reference trace, the acquired semblance spectra can get an obvious higher resolution, which is picking friendly. The proposed approach can also be combined with the AB semblance with an increased resolution and ability for handling AVO anomalies. Three kinds of synthetic example and two field data examples demonstrate the performance of our proposed approach.

ACKNOWLEDGMENTS

We would like to thank Jingye Li, Jiang Yuan, Zhaoyu Jin, Keling Chen, Pan Deng, James Rickett, Jonathan Blair Ajo-Franklin and two anonymous reviewers for helpful comments and suggestions. Yangkang Chen would like to thank Sergey Fomel for inspiring discussions on the local similarity algorithm and the Texas Consortium for Computational Seismology (TCCS) for financial support. This paper and all the figures are prepared with the Madagascar software package, which is an open-source research environment for reproducible computational experiments (Fomel et al., 2013).

APPENDIX: REVIEW OF AB SEMBLANCE

Suppose that the weight $w(j,k)$ in equation 2 has a trend of trace amplitude $a(j,k)$,

$$w(j,k) = A(j) + B(j)\phi(j,k), \tag{A-1}$$

where $\phi(j,k)$ is a known function, and $A(j)$ and $B(j)$ are two coefficients. In the simplest form, $\phi(j,k)$ can be chosen as the offset at trace k. In order to estimate $A(j)$ and $B(j)$, we can turn to minimize the following objection function of misfit between the trend and trace

amplitude:

$$F_j = \sum_{k=0}^{N-1} \left(a(j,k) - A(j) - B(j)\phi(j,k)\right)^2 . \tag{A-2}$$

Taking derivatives with respect to $A(j)$ and $B(j)$ in equation A-2, setting them to zero, and solving the two linear equations, we can obtain the the following two least-squares fitting coefficients:

$$A(j) = \frac{\sum_{k=0}^{N-1} \phi(j,k) \sum_{k=0}^{N-1} a(j,k)\phi(j,k) - \sum_{k=0}^{N-1} \phi^2(j,k) \sum_{k=0}^{N-1} a(j,k)}{\left(\sum_{k=0}^{N-1} \phi(j,k)\right)^2 - N \sum_{k=0}^{N-1} \phi^2(j,k)}, \tag{A-3}$$

$$B(j) = \frac{\sum_{k=0}^{N-1} \phi(j,k) \sum_{k=0}^{N-1} a(j,k) - N \sum_{k=0}^{N-1} a(j,k)\phi(j,k)}{\left(\sum_{k=0}^{N-1} \phi(j,k)\right)^2 - N \sum_{k=0}^{N-1} \phi^2(j,k)}. \tag{A-4}$$

Substituting $w(j,k) = A(j) + B(j)\phi(j,k)$ into equation 2 leads to the AB semblance.

REFERENCES

Chen, J., C. A. Zelt, and P. Jaiswal, 2013, A case history: Application of frequency-dependent traveltime tomography and full waveform inversion to a known near-surface target: 83nd Annual International Meeting, SEG, Expanded Abstracts, 1743–1748.

Chen, Y., and S. Fomel, 2015, Random noise attenuation using local signal-and-noise orthogonalization: Geophysics, in print.

Fomel, S., 2007, Local seismic attributes: Geophysics, **72**, A29–A33.

———, 2009, Velocity analysis using AB semblance: Geophysical Prospecting, **57**, 311–321.

Fomel, S., and E. Landa, 2014, Structural uncertainty of time-migrated seismic images: Journal of Applied Geophysics, **101**, 27–30.

Fomel, S., P. Sava, I. Vlad, Y. Liu, and V. Bashkardin, 2013, Madagascar open-source software project: Journal of Open Research Software, **1**, e8.

Guitton, A., G. Ayeni, and E. Daz, 2012, Constrained full-waveform inversion by model reparameterization: Geophysics, **77**, R117R127.

Hale, D., 2009, Strcuture-oriented smoothing and semblance: Technical Report CWP-635, Center for Wave Phenomena, Colorado School of Mines.

Li, S., 2013, Wave-equation migration velocity analysis by non-stationary focusing: 83nd Annual International Meeting, SEG, Expanded Abstracts, 1110–1115.

Li, S., A. Vladimirsky, and S. Fomel, 2013, First-break traveltime tomography with the double-square-root eikonal equation: Geophysics, **78**, U89U101.

Liu, G., S. Fomel, L. Jin, and X. Chen, 2009, Stacking seismic data using local correlation: Geophysics, **74**, V43–V48.

Luo, S., and D. Hale, 2012, Velocity analysis using weighted semblance: Geophysics, **77**, U15–U22.

Neidell, N. S., and M. T. Taner, 1971, Semblance and other coherency measures for multichannel data: Geophysics, **36**, 482–297.

Noble, M., P. Thierry, C. Taillandier, and H. Calandra, 2010, High-performance 3D first-arrival traveltime tomography: The Leading Edge, **29**, 86–93.

Osypov, K., 2000, Robust refraction tomography: 70th Annnual International Meeting, SEG, Expanded Abstracts, 2032–2035.

Rutherford, S. R., and R. H. Williams, 1989, Amplitude-versus-offset variations in gas sands: Geophysics, **54**, 680–688.

Sarkar, D., J. P. Castagna, and W. Lamb, 2001, AVO and velocity analysis: Geophysics, **66**, 1284–1293.

Sava, P., and B. Biondi, 2004a, Wave-equation migration velocity analysis - I: Theory: Geophysical Prospecting, **52**, 593–606.

———, 2004b, Wave-equation migration velocity analysis - II: Subsalt imaging examples: Geophysical Prospecting, **52**, 607–623.

Taner, M. T., and F. Koehler, 1969, Velocity spectra - digital computer derivation and applications of velocity functions: Geophysics, **34**, 859–881.

Virieux, J., and S. Operto, 2009, An overview of full-waveform inversion in exploration geophysics: Geophysics, **74**, WCC1–WCC26.

Zhou, H., L. Amundsen, and G. Zhang, 2012, Fundamental issues in full waveform inversion: 82nd Annual International Meeting, SEG, Expanded Abstracts, 1–5.

Zhu, X., D. P. Sixta, and B. G. Angstman, 1992, Tomostatics: turning-ray tomography + static corrections: The Leading Edge, **11**, 15–23.